THE MORPHOLOGIC PATTERN OF THE INTRINSIC CARDIAC NEURONAL CLUSTERS IN THE RABBIT HEART: A HISTO- AND IMMUNOHISTOCHEMICAL QUANTITATIVE STUDY

Ligita Gukauskienė

Department of Biomedical Sciences, College of Panevezys
Klaipedos 29, Panevezys, LT-35215, Lithuania

Correspondence to: Ligita Gukauskiene
E-mail: ligitagu123@gmail.com; Mobile: + 370 689 45927

Abstract. The purpose of this study was to examine the distribution and the structural organization of the intrinsic cardiac neuronal clusters in the rabbit heart. Cardiac nerve structures were stained histochemically for acetylcholinesterase (AChE) in whole-mount preparations derived from 11 young and 5 old rabbits. To reveal the neurochemical phenotype of intrinsic cardiac neurons (ICNs), double labeling for tyrosine hydroxylase (TH) and choline acetyltransferase (ChAT) was performed on paraffin sections from 2 rabbits. The clusters of ICNs were localized on the heart base at the roots of the pulmonary veins and scattered on the conus arteriosus (CA). The ChAT (+) neuronal somata were predominant within neuronal clusters. The moderate statistical significant ($P<0.05$) correlation between the cluster area and number of the ICNs was determined within both the compact ($R=0.7$) and the scattered ($R=0.8$) clusters. The total number of the ICNs on the heart base was 2013 ± 120, on average, and ranged from 1312 to 2723. The differences in the mean number of neuronal clusters, in the mean neuron number per cluster, and in the mean neuron number on the heart base were statistically insignificant between young and old rabbits ($P>0.05$). These findings demonstrate the neuronal clusters, involved about two thousands of ChAT immunoreactive neurons, predominantly distributed on the heart base near the roots of pulmonary veins, and suggest that the distribution and the morphology of the rabbit neuronal clusters correspond to the mouse and rat hearts.

Keywords: intrinsic cardiac neurons, intrinsic cardiac nervous system, rabbit, heart, acetylcholinesterase, choline acetyltransferase.

Introduction

It is thought that the sudden death of many domestic rabbits is a result of a heart attack brought on by scare. A heart attack, or myocardial infarction can be caused by a spasm of a coronary artery reducing the blood supply to the heart muscle. Moreover, both the tachycardias and the arrythmias have occurred in the rabbits and were treated by veterinarians with some success (Smith, 2003). The intrinsic cardiac nervous system is a crucial regulator of the coronary blood flow as well as the cardiac chronotropic, dromotropic and inotropic functions (Tsuboi et al., 2000; Zong et al., 2004; Setty et al., 2008). However, the detailed morphology of the rabbit intrinsic cardiac nervous system so far has not been in a scope of the special investigations.

The vertebrate cardiac ganglia or the neuronal clusters contain the ICNs that were initially regarded as simple relay stations in the vagal efferent pathway to the heart. Although it has been proposed that the ICNs work as an integrative nerve centres modulating extrinsic autonomic inputs from the spinal cord, brain stem, and insular cortex as well as mediates local cardio-cardiac reflexes (Arora et al., 2000; Armour, 2008). The recent findings demonstrate that the vertebral ICNs have a complex neurochemical anatomy (Hoard et al., 2008; Hoover et al., 2009). This includes the presence of a dual cholinergic/nitrergic phenotype for most ICNs as well as the presence of noradrenergic markers in subpopulations of the ICNs (Hoover et al., 2009). Lastly, the recent report shows that vertebral ICNs receive a plethora of the non-cholinergic inputs that include nerve fibers stained for VIP, CGRP, SP, nNOS, and noradrenergic markers, and provide neuroanatomical support for the integrative capacity of these ICNs (Hoover et al., 2009).

The number of the ICNs was used to describe quantitatively intrinsic cardiac nerve plexus in many animal species, including the human (de Souza et al., 1996; Akamatsu et al., 1999; Pauza et al., 2002; Batulevicius et al., 2003; Jurgaitiene et al., 2004; Batulevicius et al., 2005; Batulevicius et al., 2012). The number of the ICNs may be decreased through several factors such as aging, diabetes and infectious diseases such as the Chagas disease (Kamal et al., 1991; Akamatsu et al., 1999; Ribeiro et al., 2002; Rodrigues et al., 2002; Jurgaitiene et al., 2004; Gama et al., 2010). Many cardiovascular reflexes are reduced in aged animals (Franchini et al., 1996). Therefore, increased fundamental understanding of the physiology and morphology of the rabbit intrinsic cardiac nervous system is critically important.

The distribution and architecture of the rabbit intrinsic cardiac ganglia are rather poorly examined. Therefore, the aim of the present study was to (1) examine the distribution of the intrinsic cardiac neuronal clusters in the rabbit heart; (2) determine the structural organization of the rabbit intrinsic cardiac neuronal clusters; (3) assess the number of the intrinsic cardiac neurons.

Materials and Methods

The study was performed on thirteen juvenile and five

old Californian rabbits of either gender. Young animals were 2–6 month old and weighed 2.6±0.4 kg, while old animals were 3–4 years old and weighed 4.9±0.2 kg. The animals were anesthetized with a lethal dose of sodium thiopental (30 mg/kg i.v) in accordance with local and state guidelines for the care and use of the laboratory animals (Permission No. 0206).

Whole-mount preparations. After euthanasia, the rabbit chest was opened and the heart was perfused with 0.01 M phosphate-buffered saline (PBS; 0.9% NaCl, pH 7.4), via a cannula inserted into the left ventricular cavity. To perform the quantitative analysis of ICNs, the histochemistry for AChE was carried out on sixteen whole-mounts rabbit heart preparations. After perfusion with 0.01 M PBS at room temperature, hearts were removed from the chest and placed into a dissecting dish containing 0.01 M PBS. The walls of the atria and interatrial septum were separated from ventricles, the septum was trimmed free of the atrial walls, and the atrial tissue was pinned flat on the dissecting dish. In order to count the ventricular neurons, the wall of the conus arteriosus was cut and pinned flat on the dissecting dish.

Histochemistry. The prepared whole-mount heart preparations were prefixed for 30 minutes at 4°C in 4 % paraformaldehyde solution in 0.01 M phosphate buffer (pH 7.4). After prefixation, the heart preparations were washed for 12 h at 4°C in 0.01 M PBS containing hyaluronidase (0.5 mg/100 ml, Sigma-Aldrich Inc., St Louis, MO, USA) and placed for 4 h at 4°C in Karnovsky-Roots medium as described previously (Pauza et al., 1999). Whole-mount heart preparations stained for AChE were fixed for 96 h period at 4 % paraformaldehyde solution in 0.01 M phosphate buffer (pH 7.4). After fixation the whole-mount preparations were dehydratated with 50-minute washes through a graded ethanol series, immersed for 2 h period in xylene (Sigma-Aldrich Inc., St Louis, MO, USA), mounted with a Roti®-Histokitt mounting medium (Carl Roth, Karlsruhe, Germany), and slipped.

Heart sections. In order to reveal the neurochemical phenotype of cardiac neurons within main clusters, double labeling for TH and ChAT (Table 1) was performed on paraffin sections as described previously (Pauza et al., 2013). Thereafter the specimens were again washed in 0.01M PBS, and mounted in Vectashield Mounting Medium (Vector Laboratories, California, U.S.A.). A cover slip was placed on the tissue and then sealed with clear nail polish. Both positive and negative controls were used.

Table 1. **Primary and secondary antisera used in the study**

Antigen	Host	Dilution	Supplier	Catalog number
Primary				
TH	Mouse	1:500	Invitrogen[a]	32-2100
CHAT	Goat	1:100	Chemicon[b]	AB 144P
Secondary				
Mouse^{FITC}	Donkey	1:100	ImmunoStar[c]	715-095-151
Goat^{Cy3}	Donkey	1:300	Chemicon[b]	AP 180C

[a] Invitrogen Corporation, Flynn Rd, Camarillo, CA; [b] Chemicon International, Temecula, California, USA; [c] ImmunoStar Incorporation, Wisconsin, USA; Jackson ImmunoResearch Europe Ltd., Suffolk, UK.

Microscopic examination and quantitative analysis. To examine the area, shape of the neuronal cluster and the number of neuronal somata (with clearly visible nuclei), the whole mounts preparations stained histochemically for AChE were analyzed using an AxioImager M1 bright field microscope (Zeiss, Jena, Germany). Two independent investigators performed the control measurements of three clusters per whole mount (n=11). The result error of both investigators was 6±1%. The heart sections stained immunohistochemically were analyzed utilizing an AxioImager Z1 fluorescence microscope (Zeiss, Gottingen, Germany) equipped with a set of the filters to observe the fluorescein isothiocyanate (FITC) and cyanine (Cy3) fluorescence, an Apotome (Zeiss, Jena, Germany) and digital monochrome camera AxioCam MRm (Zeiss, Gottingen, Germany). The adjustments of the final images and measurements of cardiac neural structures were performed using AxioVision 4.8.1 software (Zeiss, Jena, Germany).

Statistical analysis. Data were processed using the Origin Lab software version 6.1 (OriginLab Corporation, Northampton, MA, USA). Data shown both in the text and table are expressed as mean ± standard error of mean (SEM). Statistical significance of the difference between the means was performed with Student's paired and independent tests. Differences were considered statistically significant at $P<0.05$.

Results

In all the examined whole-mounts of the rabbit atria, the ICNs were topographically related to the particular nerve plexus of heart hilum (NPHH) on the heart base and were concentrated into four main neuronal cluster groups situated within the venous part of the heart hilum: (1) at the cranial aspect of the interatrial groove (the septal cranial (SCr) group); (2) on the medial wall of the right cranial vein root (the right cranial (RCr) group); (3) ventrally to the left pulmonary vein (LPV) root (the left cranial (LCr) group); (4) between the middle pulmonary (MPV) and caudal cava vein roots (the septal caudal (SCd) group) (Fig. 1). In the present study, the groups of the neuronal clusters have been named according to their topography, and were regularly found in every heart examined, except the RCr cluster group that was

identified only in half of examined preparations. In all the examined ventricular whole-mount preparations, the solitary small ventricular clusters (VCs) of ICNs were scattered nearby the pulmonary trunk (PT) and distributed on the CA (Fig. 2b, c).

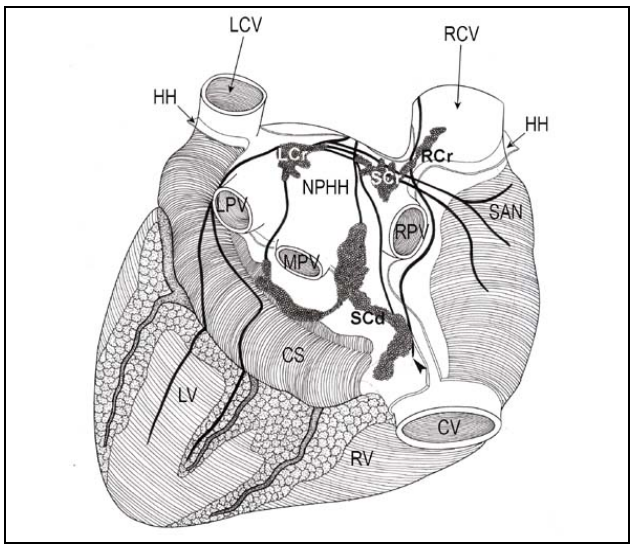

Fig 1. **Drawing of the dorso-cranial view of the rabbit heart illustrating the distribution of the intrinsic cardiac neuronal clusters within the nerve plexus of the heart hilum (NPHH). The nerve plexus and neuronal clusters were outlined from the whole-mount preparations of the rabbit atria stained histochemically for AChE. The black arrowhead points to nerves that penetrate into interatrial septum towards the atrioventricular nodal (AVN) region. The bubbled polygonal areas show the intrinsic cardiac neuronal clusters, the thin wiggle lines - nerves of the NPHH. Abbreviations: CS – coronary sinus; CV – caudal cava vein; HH – heart hilum; LCr - left cranial cluster group; LCV – left cranial cava vein; LPV - left pulmonary vein; LV – left ventricle; MPV - middle pulmonary vein; RCr – right cranial cluster group; RCV – right cranial cava vein; RPV – right pulmonary vein; RV – right ventricle; SAN – sinoatrial nodal region; SCd – septal caudal cluster group; SCr – septal cranial cluster group.**

The neuronal cluster groups contained one or two principal large clusters (in terms of both area and number of the ICNs) interconnected with the numerous small accessory clusters via thin nerve bundles (Fig. 2a). The principal clusters were easily discernible with the naked eye and were regularly situated at the junctions of the nerve bundles or nerves (Fig. 2a). The accessory clusters comprising about 73% of all the examined clusters were frequently located along the course of the nerve bundles or nerves (Fig. 2a). The both types of clusters, the principal and accessory, did vary in their shape, but most have the irregular form because of their extensions at the sites where nerves connected to a cluster (Fig. 2). In all the examined whole-mounts, the unilayered clusters were predominantly distributed on the heart base and CA (Fig. 2).

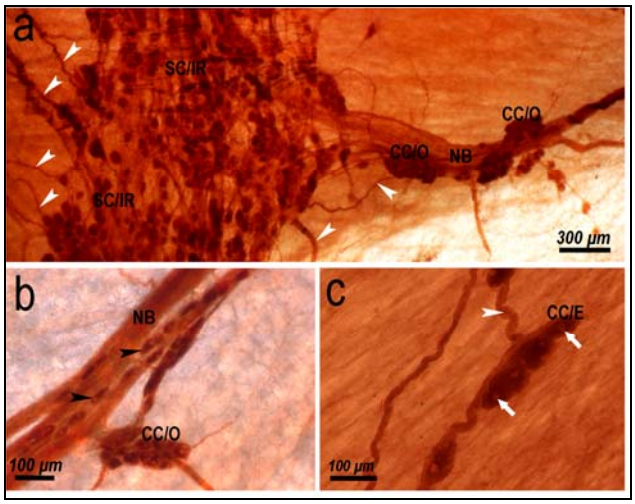

Fig 2. **The micrographs of the rabbit intrinsic neuronal clusters stained histochemically for AChE demonstrating the structural organization of scattered, compact, irregular, oval and elongated clusters distributed within rabbit atrial (a) and ventricular (b, c) whole-mount preparations. Note the large principal irregular scattered cluster and three accessory oval compact clusters located along the nerve bundle (a) panel as well as oval compact cluster situated at the crossection of nerve bundles and single neurons distributed along the nerve bundle (b) pannel. White arrowheads indicate the nerves, black arrowheads demonstrate the single neurons, white solid arrows indicate the nuclei of neurons. Abbreviations: CC/E – compact cluster elongated; CC/O – compact cluster oval; NB – nerve bundle; SC/IR – scattered cluster irregular.**

The neuronal somata in the unilayered cluster were regularly packed one close to another forming the predominant compact type of the neuronal cluster (Fig. 2). However, the ICNs within the compact cluster were easily discernible by a light microscope (Fig. 2). The sparsely arranged neurons were identified within a single scattered principal clusters distributed in the SCr, LCr and SCd groups. On average, the area of the principal compact cluster was 0.43±0.1 mm^2 and ranged from 0.01 to 2.08 mm^2. The neuronal number of the principal compact cluster was 294±56 and ranged between 3 and 728 neurons. The area of the scattered cluster was 0.65±0.1 mm^2 and ranged from 0.22 to 1.64 mm^2. On average, the scattered cluster involved up to 472±54 neurons, and the number of the ICNs ranged from 194 to 728 within scattered cluster. The moderate statistical significant ($P<0.05$) correlation between the cluster area and number of the ICNs was determined within both the compact ($R=0.7$) and the scattered ($R=0.8$) clusters (Fig. 3). On average, the number of the neuronal somata of the accessory cluster was 13±1, and it ranged between 2 and 228 neurons. The ventricular clusters were small and involved on average 31±5 neuronal somata. The neuron number of the ventricular cluster ranged from 6 to 69. The mean number of the VCs was 15±5, and ranged from 1 to

34. Although the rabbit ICNs were mostly cumulated into the neuronal clusters, the large amount of the single neurons involved up to 50 % of all ventricular ICNs was identified on the CA. On the heart base, there were found only 15 % of all atrial ICNs.

Double immunostaining for ChAT and TH revealed that the rabbit intrinsic cardiac neuronal clusters consisted of the ChAT immunoreactive neuronal somata surrounded by baskets of the varicose nerve terminals that expressed ChAT more intensely than the neuronal somata (Fig. 4).

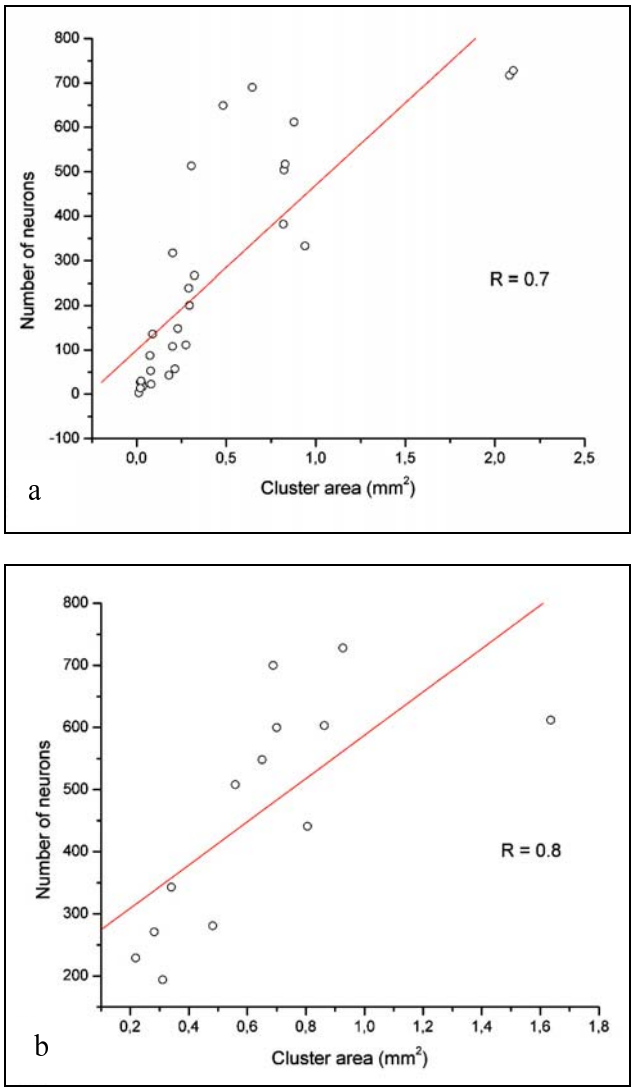

Fig 3. **The correlation between the area of neuronal cluster and the number of the intrinsic cardiac neurons within compact (a) and scattered (b) cluster. R - correlation coefficient at P<0.05.**

In all examined animals, the total number of the ICNs on heart base was 2013±120, on average, and ranged from 1312 to 2723 (Table 2). Approximately, there were concentrated about 700 ICNs within neuronal clusters related to anatomically via epicardial nerves to the sinoatrial node, about 1000 ICNs resided within neuronal clusters related to the atrioventricular node, and 100 neurons were related via epicardial nerves to the contractile myocardium and coronary arteries (Table 2). The young individuals contained 2025±141 neuronal somata on the heart base, while the total number of the ICNs on the heart base of the old animals was 1968±268 (Table 2). The mean number of the neuronal clusters was 52±3 in the juvenile animals and 37±6 in the old animals (Table 2). The mean neuron number per cluster was 37±5 in the young animals and 47±12 in the old animals (Table 2). The differences in the mean number of the neuronal clusters, in the mean neuron number per cluster, and in the mean neuron number on the heart base were statistically insignificant between the young and old rabbits (P>0.05). In all the examined individuals, the number of neuron clusters, the neuron number per cluster, and the neuron number on the heart base varied from heart to heart (Table 2).

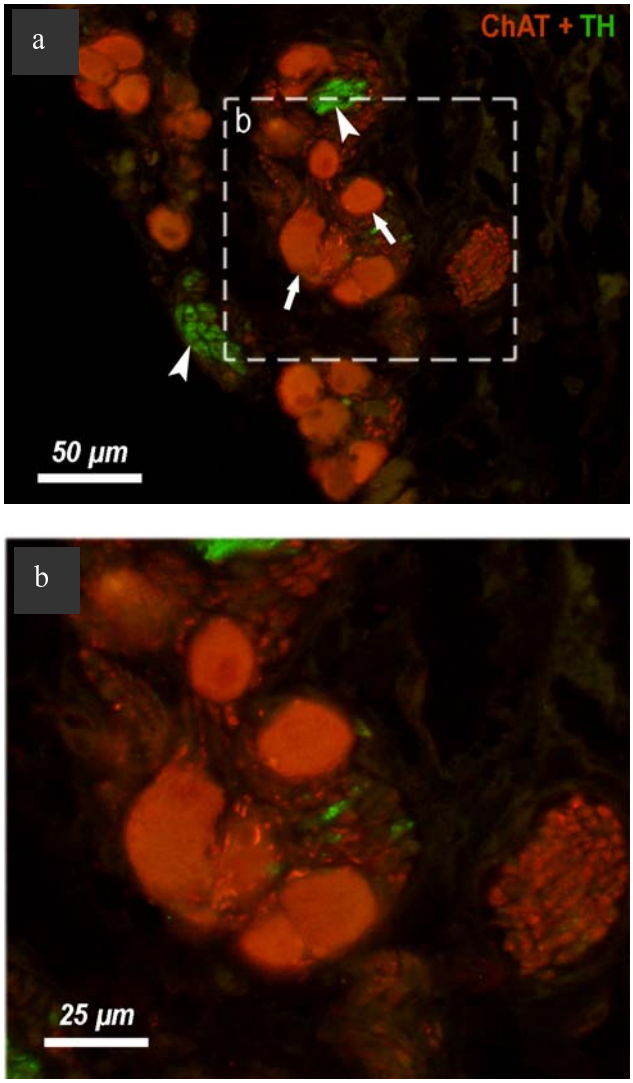

Fig 4. **Micrographs of the paraffin section of the rabbit atrial wall to demonstrate the TH (green), ChAT (red) immunoreactive nerve fibers and neuronal somata. White arrowheads point nerve fibers, white thin arrows point - neuronal somata. The boxed area in a panel is enlarged as b panel.**

Table 2. **The number of neuronal clusters and neuronal somata in the rabbit HB**

Group of neuronal clusters within heart base (HB)	N	Number of clusters		Neuron number per cluster		Neuron number on HB	
		Mean	Range	Mean	Range	Mean	Range
Juvenile individuals							
Clusters related to the SAN region							
Right cranial group	7	3±1	0–8	17±6	2–101	71±43	3–239
Septal cranial group	11	11±1	3–18	55±13	2–728	608±80	141–940
Clusters related to the AVN region							
Septal caudal group	11	23±3	7–35	27±6	2–394	567±95	149–1203
Left cranial group	7	14±2	4–24	33±7	2–643	565±105	123–1394
The single neurons of HB	10	–	–	–	–	304±58	133–576
In average on HB	–	52±3	38–64	37±5	2–728	2025±141	1312–2723
Old adult individuals							
Clusters related to the SAN region							
Right cranial group	4	1±1	0–2	7±2	3–11	10±4	6–14
Septal cranial group	3	13±5	8–18	54±26	2–756	788±125	663–912
Clusters related to the AVN region							
Septal caudal group	5	17±3	11–21	37±14	2–614	624±84	495–781
Left cranial group	4	8±2	5–12	66±32	2–690	544±80	439–702
The single neurons of HB	5	–	–	–	–	203±43	128–280
In average on HB	–	37±6	25–46	47±12	2–756	1968±268	1433–2256
All individuals on HB	–	48±3	25–64	40±5	2–756	2013±120	1312–2723

Abbreviations: AVN – atrioventricular node; HB – heart base; LCr – left cranial cluster; N - number of checked whole mounts; RCr – right cranial cluster; SAN – sinoatrial node; SCd – septal caudal cluster; SCr – septal cranial cluster.

Discussion

The present investigation addresses the neurotopography and neuromorphology of the ICNs clusters in the whole-mount preparations of the rabbit heart using histochemical AChE staining. The results of this study demonstrate the topography of the ICNs, the morphology of the ICNs clusters, the neurochemical phenotype and the number of the ICNs within rabbit heart hilum, and age-related changes on the ICNs.

In this study, the double immunostaining for ChAT and TH revealed that the rabbit intrinsic cardiac neuronal clusters consisted of the ChAT immunoreactive neuronal somata surrounded by baskets of the varicose nerve terminals that expressed ChAT more intensely than the neuronal somata. The predominant cholinergic phenotype of the ICNs has been earlier demonstrated employing a histochemistry for AChE as well as immunohistochemistry for ChAT in the mouse, rat, rabbit, dog, and human (Bojsen-Moller and Tranum-Jensen, 1972; Pauza et al., 2002; Rysevaite et al., 2011b).

The present data showed that the ICNs were topographically related to the particular nerve plexus of the heart hilum (NPHH) on the heart base and were concentrated into four main neuronal cluster groups which situated within the venous part of the heart hilum: (1) at the cranial aspect of the interatrial groove; (2) on the medial wall of the right cranial vein root; (3) ventrally to the left pulmonary vein root; and (4) between the middle pulmonary and caudal cava vein roots. In the rabbits, rats and mice, the neuronal cluster groups anatomically related to the NPHH are distributed at approximately the same locations of the heart hilum (i.e. at the cranial aspect of the interatrial groove, medially to the right and left cranial cava vein roots), and epicardially below the LPV and MPV roots (Batulevicius et al., 2003; Rysevaite et al., 2011a). The present observations are in contrast with the previous data (Batulevicius et al., 2003; Rysevaite et al., 2011a) concerning the VCs distributed near the PT on the CA. The hearts of the rats and mice lacked the ICNs scattered onto ventral surface of the ventricles.

In the present study, it has been estimated that approximatelly 1300–2700 intrinsic neurons are involved in the rabbit heart hilum. The approximated data demonstrate that on average 700 ICNs concentrate within neuronal clusters anatomically related via epicardial nerves to the sinoatrial nodal region, 1000 neurons reside within neuronal clusters related to the atrioventricular nodal region, and 100 neurons are related via epicardial nerves to the contractile myocardium and coronary arteries. The results of the neuronal count in cardiac sections and whole-mount preparations of the mouse and rat hearts do contradict to these findings. The reports by Pardini et al. (1987) and Batulevicius et al. (2003), who counted neurons in tissue sections, indicate about 4000–7000 neurons residing within neuronal clusters of the rat heart. In sharp contrast, de Souza et al. (1996), Acamatsu et al. (1999) and Rysevaite et al. (2011b) counting the neurons in whole-mount preparations found only 1000–2000 ICNs in the hearts of rat and mouse. The method based on neuronal counts in the whole-mount preparations, however, allows even approximate estimation of neuronal number because many ICNs in the rats and mice are densely packed one above another, and neurons within these clusters are poorly discernible even by a light microscope. These findings do contradict to

previous information, and demonstrate the rabbit ICNs sparsely clustered within unilayered clusters.

The present study demonstrates insignificant differences in the mean number of the neuronal clusters, in the mean neuron number per cluster, and in the mean neuron number per heart hilum between the young and old individuals. With respect to the age-related decrease of the neuronal number, the present data correspond to the findings in the rat and guinea-pig hearts (Batulevicius et al., 2003, 2005), but contrast with the previous report on the human and canine hearts that demonstrated remarkable age-related decrease in the number of the ICNs (Pauza et al., 2002). In general, the insignificant age-related differences of the neuron number in the rabbit, rat and guinea-pig hearts might indicate that the hearts of the rodents and lagomorphs, unlike the human and canine hearts, do not undergo a decrease in neuronal number with aging (Batulevicius et al., 2005). Regarding the age-related degeneration of the nerve structures in the rodent heart, the significant reduce of the total numbers of the vagal efferent cardiac axons and basket endings was reported in the aged rats (Ai et al., 2007).

Contrary to the rabbit ICNs, the human, canine, porcine, sheep and other large animal ICNs are arranged into the numerous ganglia (Pauza et al., 2002). Serial confocal sections through those ganglia as well as routine histology revealed that neuronal somata were distributed in the periphery of the ganglion adjacent to the well-defined fibrous capsule (Arora et al., 2003). The interior of those ganglia was comprised of neuropil, with numerous dendrites of the peripherally located neurons or small nerves (Arora et al., 2003; Pauziene and Pauza, 2003). Physiological studies have shown that some numerous ganglia of the large mammals serve as additional centre's for divergention of the cardiac inputs and may affect the parasympathetic control of the cardiac rate and conduction through an intracardiac neuronal circuits, which thereby indirectly modulates the actions to the sinoatrial and the atrioventricular nodes (Gatti et al., 1995; Gray et al., 2004).

These findings demonstrate the neuronal clusters that involved about two thousands of the ChAT immunoreactive neurons, predominantly distributed on the heart base near the roots of pulmonary veins, and suggest that the distribution and the morphology of the rabbit neuronal clusters correspond to the mouse and rat hearts. The present data provide fundamental anatomical basis for further immunohistochemical, electron microscopic investigations, physiological experiments and contain pivotal importance for treatment of the rabbit cardiac diseases.

Acknowledgements

The author sincerely thanks Mr. Šarunas Janavičius and Lithuanian Fur and Rabbits Breeders Association, for providing material for this study.

References

1. Ai J., Gozal D., Li L., Wead WB., Chapleau MW., Wurster R., Yang B., Li H., Liu R., Cheng Z. Degeneration of vagal efferent axons and terminals in cardiac ganglia of aged rats. J Comp Neurol. 2007. 504. P. 74–88.

2. Akamatsu FE., De-Souza RR., Liberti EA. Fall in the number of intracardiac neurons in aging rats. Mech Ageing Dev. 1999. 109. P. 153–161.

3. Armour JA. Potential clinical relevance of the 'little brain' on the mammalian heart. Exp Physiol. 2008. 93. P. 165–176.

4. Arora RC., Ardell JL., Armour JA. Cardiac Denervation and Cardiac Function. Curr Interv Cardiol Rep. 2000. 2. P. 188–195.

5. Arora RC., Waldmann M., Hopkins DA., Armour JA. Porcine intrinsic cardiac ganglia. Anat Rec. 2003. 271. P. 249–258.

6. Batulevicius D., Pauziene N., Pauza DH. Topographic morphology and age-related analysis of the neuronal number of the rat intracardiac nerve plexus. Ann Anat. 2003. 185. P. 449–459.

7. Batulevicius D., Pauziene N., Pauza DH. Architecture and age-related analysis of the neuronal number of the guinea pig intrinsic cardiac nerve plexus. Ann Anat. 2005. 187. P. 225–243.

8. Batulevicius D., Skripkiene G., Batuleviciene V., Skripka V., Dabuzinskiene A., Pauza DH. Distribution, structure and projections of the frog intracardiac neurons. Auton Neurosci. 2012. 168. P. 14–24.

9. Bojsen-Moller F., Tranum-Jensen J. Rabbit heart nodal tissue, sinuatrial ring bundle and atrioventricular connexions indentified as a neuromuscular system. J Anat. 1972. 112. P. 367–382.

10. de Souza RR., Gama EF., de Carvalho CA., Liberti EA. Quantitative study and architecture of nerves and ganglia of the rat heart. Acta Anat. 1996. 156. P. 53–60.

11. Franchini KG., Moreira ED., Ida F., Krieger EM. Alterations in the cardiovascular control by the chemoreflex and the baroreflex in old rats. The Am J Physiol. 1996. 270. P. 310–313.

12. Gama EF., Santarem JM., Liberti EA., Jacob Filho W., Souza RR. Exercise changes the size of cardiac neurons and protects them from age-related neurodegeneration. Ann Anat. 2010. 192. P. 52–57.

13. Gatti PJ., Johnson TA., Phan P., Jordan IK., 3rd, Coleman W., Massari VJ. The physiological and anatomical demonstration of functionally selective parasympathetic ganglia located in discrete fat pads on the feline myocardium. J Auton Neurosci. 1995. 51. P. 255–259.

14. Gray AL., Johnson TA., Ardell JL., Massari VJ. Parasympathetic control of the heart. II. A novel interganglionic intrinsic cardiac circuit mediates neural control of heart rate. J Appl Physiol. 2004. 96. P. 2273–2278.

15. Hoard JL., Hoover DB., Mabe AM., Blakely RD., Feng N., Paolocci N. Cholinergic neurons of mouse intrinsic cardiac ganglia contain noradrenergic enzymes, norepinephrine transporters, and the neurotrophin receptors tropomyosin-related kinase A and p75. Neuroscience. 2008. 156. P. 129–142.

16. Hoover DB., Isaacs ER., Jacques F., Hoard JL., Page P., Armour JA. Localization of multiple neurotransmitters in surgically derived specimens of human atrial ganglia. Neuroscience 2009. 164. P. 1170–1179.

17. Jurgaitiene R., Pauziene N., Azelis V., Zurauskas E. Morphometric study of age-related changes in the human intracardiac ganglia. Medicina (Kaunas) 2004. 40. P. 574–581.

18. Kamal AA., Tay SS., Wong WC. The cardiac ganglia in streptozotocin-induced diabetic rats. Arch Histol Cytol. 1991. 54. P. 41–49.

19. Pardini BJ., Patel KP., Schmid PG., Lund DD. Location, distribution and projections of intracardiac ganglion cells in the rat. J Auton Neurosci. 1987. 20. P. 91–101.

20. Pauza DH., Pauziene N., Pakeltyte G., Stropus R. Comparative quantitative study of the intrinsic cardiac ganglia and neurons in the rat, guinea pig, dog and human as revealed by histochemical staining for acetylcholinesterase. Ann Anat. 2002. 184. P. 125–136.

21. Pauza DH., Saburkina I., Rysevaite K., Inokaitis H., Jokubauskas M., Jalife J., Pauziene N. Neuroanatomy of the murine cardiac conduction system: A combined stereomicroscopic and fluorescence immunohistochemical study. Auton Neurosci. 2013. http://dx.doi.org/10.1016/j.autneu.2013.01.006.

22. Pauza DH., Skripka V., Pauziene N., Stropus R. Anatomical study of the neural ganglionated plexus in the canine right atrium: implications for selective denervation and electrophysiology of the sinoatrial node in dog. Anat Rec. 1999. 255. P. 271-294.

23. Pauziene N., Pauza DH. Electron microscopic study of intrinsic cardiac ganglia in the adult human. Ann Anat. 2003. 185. P. 135–148.

24. Ribeiro LC., Barbosa AA., Jr., Andrade ZA. Pathology of intracardiac nerves in experimental Chagas disease. Mem I Oswaldo Cruz. 2002. 97. P. 1019–1025.

25. Rodrigues E., Liberti EA., Maifrino LB., de Souza RR. Cardiac denervation in mice infected with Trypanosoma cruzi. Ann Trop Med Parasit. 2002. 96. P. 125–130.

26. Rysevaite K., Saburkina I., Pauziene N., Noujaim SF., Jalife J., Pauza DH. Morphologic pattern of the intrinsic ganglionated nerve plexus in mouse heart. Heart rhythm. 2011a. 8. P. 448–454.

27. Rysevaite K., Saburkina I., Pauziene N., Vaitkevicius R., Noujaim SF., Jalife J., Pauza DH. Immunohistochemical characterization of the intrinsic cardiac neural plexus in whole-mount mouse heart preparations. Heart rhythm. 2011b. 8. P. 731–738.

28. Setty S., Zong P., Sun W., Tune JD., Downey HF. Hypoxia-induced vasodilation in the right coronary circulation of conscious dogs: role of adrenergic activation. Auton Neurosci. 2008. 138. P. 76–82.

29. Kathryn R. Smith. Rabbit Health in the 21st Century. Second Edition. A Guide for Bunny Parents. USA. 2003. P. 104–106.

30. Tsuboi M., Furukawa Y., Nakajima K., Kurogouchi F., Chiba S. Inotropic, chronotropic, and dromotropic effects mediated via parasympathetic ganglia in the dog heart. Am J Physiol. 2000. 279. P. H1201–1207.

31. Zong P., Sun W., Setty S., Tune JD., Downey HF. Alpha-adrenergic vasoconstrictor tone limits right coronary blood flow in exercising dogs. Exp Biol Med (Maywood). 2004. 229. P. 312–322.

Received 13 March 2013
Accepted 2 October 2013